Effects of Non-Gaussian Parameters and Texture Angle on the Hydrodynamic Lubrication of Cross-Hatched Surfaces

Miao Liu[1], Yawen Fan[2,*], Jingfeng Shen[1,*]
[1]*School of Mechanical Engineering, University of Shanghai for Science and Technology, Shanghai , China*
[2]*Sino-British International College, University of Shanghai for Science and Technology, Shanghai, China*
**Corresponding Author*

Abstract: After honing, the surfaces of key friction pairs, such as internal combustion engine cylinder liners, exhibit pronounced non-Gaussian distribution characteristics, making it difficult for traditional lubrication models based on Gaussian assumptions to accurately predict their actual tribological performance. To address this issue, a numerical-simulation-based method for surface topography optimization is proposed. A digital simulation framework integrating the Johnson transformation system with a deterministic Reynolds equation solver is established. On the basis of accurate reconstruction of engineering surfaces and decoupling of statistical characteristics, the nonlinear effects of the non-Gaussian parameters, namely skewness and kurtosis, together with texture angle, on hydrodynamic lubrication performance are systematically quantified. The results show that surface skewness is the key parameter governing lubrication performance. When the skewness is S_{sk} ≈-1.0 and the kurtosis is $S_{ku} \approx 4$, the surface exhibits an ideal plateau–valley morphology, which enhances the micro-hydrodynamic effect while maintaining optimal oil-retention capacity. In terms of texture orientation, a 60° cross-hatched texture is more likely to form a hydrodynamic convergence center than the conventional 45° texture, thereby providing greater load-carrying potential. In addition, although the optimized non-Gaussian surface exhibits a slightly lower steady-state load-carrying capacity than the Gaussian surface under full-film lubrication, its characteristic deep valleys act as micro oil reservoirs, significantly improving the anti-scuffing robustness of the friction pair under starved or mixed lubrication conditions. This study provides theoretical support for the forward design of surface textures for high-performance friction pairs.

Keywords: Non-Gaussian Surfaces; Hydrodynamic Lubrication; Numerical Simulation; Surface Texturing; Texture Angle

1. Introduction

Friction and wear are the primary causes of energy dissipation and failure in mechanical systems. In key friction pairs such as cylinder liner–piston ring pairs in internal combustion engines and radial journal bearings, surface topography plays a key role in the formation and load-carrying capacity of the oil film [1]. With the development of precision manufacturing technologies, the performance requirements for mechanical components have become increasingly stringent. Improving tribological performance through active design and control of surface micro-textures has become a major research focus in the field of surface engineering [2]. Especially in heavy-duty diesel engines, the cylinder liner-piston ring friction pair operates under extreme conditions of high temperature and high burst pressure, making it highly susceptible to oil film rupture. As shown in Figure 1, the failed surface retains a cross-honed texture of approximately 58°. Although this specific texture angle is widely used in engineering, its traditional surface topography clearly fails to provide sufficient lubricant retention capacity to prevent damage propagation under extremely starved lubrication conditions. This indicates that relying solely on traditional honing angle design is no longer sufficient to meet the demands of increasingly severe operating conditions, and new topographic description

parameters, such as non-Gaussian statistical features, must be introduced for deeper optimization. Therefore, optimizing the surface micro-topography for such harsh conditions and utilizing texture features to store lubricating oil to prevent cylinder scoring is of great engineering significance

Figure 1. Morphology of Scuffing Damage in Heavy-Duty Cylinder Liners Caused by Lubrication Failure [3]

Traditionally, classical contact mechanics theories represented by the Greenwood-Williamson (GW) model and the Patir-Cheng average flow model [4] have dominated rough surface research. These theories typically assume that surface roughness heights follow a Gaussian normal distribution, where the skewness is S_{sk}=0 and the kurtosis is $S_{ku} = 3$. However, actual engineering surfaces strongly influenced by machining processes such as turning, grinding, and honing often exhibit significant non-Gaussian characteristics. For instance, the inner wall of a plateau-honed cylinder liner [5] exhibits negative skewness ($S_{sk} < 0$) and a typical plateau–deep-valley morphology, and this non-Gaussian topography is considered to have excellent oil retention and load-carrying capacities [6]. Ignoring these non-Gaussian features can lead to prediction errors exceeding 10% for maximum oil film pressure and load-carrying capacity.

Furthermore, traditional surface texture research heavily relies on physical experiments, which involve machining solid samples and testing them on tribometers. This approach has drawbacks such as high costs, long cycles, and the difficulty of independently controlling a single statistical parameter (e.g., maintaining constant skewness while changing roughness) [7].

To address the above issues, numerical simulation techniques have emerged. These techniques enable the generation of virtual surfaces with precisely controllable statistical features and the prediction of their performance through multiphysics simulations, thereby reducing reliance on costly physical trial-and-error processes [8]. In this study, a numerical simulation framework integrating surface generation, virtual validation, and performance evaluation is established. Based on the algorithm proposed by Ma et al. [9], non-Gaussian cross-hatched surfaces are reconstructed using the Johnson transformation system [10]. Using a deterministic Reynolds equation solver, this study systematically investigates the nonlinear effects of skewness, kurtosis, and texture angle on hydrodynamic lubrication performance, identifies optimal surface topography parameters, and provides theoretical guidance for the digital design of high-performance friction pairs.

2. Numerical Methods and Calculation Principles

2.1 Digital Reconstruction of Non-Gaussian Cross-Hatched Surfaces

This study adopts a hybrid algorithm based on digital filtering and probability transformation to generate engineering surfaces with specific statistical features. This method is mainly divided into two stages: the generation of anisotropic Gaussian random fields and the non-Gaussian probability mapping.

2.1.1 Generation of anisotropic gaussian random fields

First, the Fast Fourier Transform (FFT) technique is used to generate a Gaussian rough surface that satisfies a specific Autocorrelation Function (ACF). "For engineering surfaces with texture directionality (such as cylinder liners) the spatial correlation is described by an exponential ACF:

$$R(x,y) = \sigma^2 \exp\left(-2.3\sqrt{\left(\frac{x'}{\beta_x}\right)^2 + \left(\frac{y'}{\beta_y}\right)^2}\right) \quad (1)$$

Where σ is the root mean square roughness, and β_x and β_y are the correlation lengths along the primary and secondary texture axes, respectively. To simulate the texture angle θ, a coordinate rotation transformation is introduced:

$$\begin{cases} x' = x\cos\theta - y\sin\theta \\ y' = x\sin\theta + y\cos\theta \end{cases} \quad (2)$$

Based on the Wiener-Khinchin theorem, the Power Spectral Density (PSD) of the surface

and the autocorrelation function form a Fourier transform pair. By filtering Gaussian white noise $\eta(k_x, k_y)$ in the frequency domain, a Gaussian surface $z_G(x, y)$ with the target spatial correlation can be obtained:

$$z_G(x, y) = \text{IFFT}\left(\text{FFT}(\eta) \cdot \sqrt{|\text{FFT}(R)|}\right) \quad (3)$$

To simulate the typical "cross-hatched" features of plateau honing, this paper uses a linear superposition method to synthesize two anisotropic surfaces with different texture directions ($+\theta$ and $-\theta$):

$$z_{cross}(x, y) = \frac{1}{2}[z_{+\theta}(x, y) + z_{-\theta}(x, y)] \quad (4)$$

2.1.2 Non-gaussian mapping based on the johnson transformation system

The generated z_{cross} follows a standard normal distribution. To introduce negative skewness (deep valleys) and high kurtosis features, the Johnson transformation system (or cumulative distribution function mapping method) is adopted to perform a non-linear transformation on the surface height. Assuming the target surface's cumulative distribution function (CDF) is F_{target}, the final non-Gaussian surface $z(x, y)$ can be obtained by:

$$z(x, y) = F_{target}^{-1}\left(\Phi\left(z_{cross}(x, y)\right)\right) \quad (5)$$

Where $\Phi(\cdot)$ is the cumulative distribution function of the standard normal distribution, and F_{target}^{-1} is the inverse function of the target non-Gaussian distribution. The target distribution is usually constructed through Gram-Charlier series expansion to accurately match the set skewness S_{sk} and kurtosis S_{ku}.

2.2 Numerical Simulation of Surface Functional Parameters

To quantify the oil retention capacity of the generated surface, this study introduces the Abbott-Firestone curve analysis. According to the ISO13565-2 standard, the following core parameters are calculated:

(1) Core roughness depth (R_k): Represents the height of the main load-bearing area of the surface.

(2) Reduced valley depth (R_{vk}): Represents the oil retention capacity of the deep valleys on the surface. For the discretized surface height sequence z_{ij}, the relationship between its probability density function $p(z)$ and the Abbott curve $Mr(c)$ is defined as:

$$Mr(c) = \int_c^{\infty} p(z)\, dz \times 100\% \quad (6)$$

Where c is the truncation height, and $Mr(c)$ is the Material Ratio.

2.3 Deterministic Hydrodynamic Lubrication Model

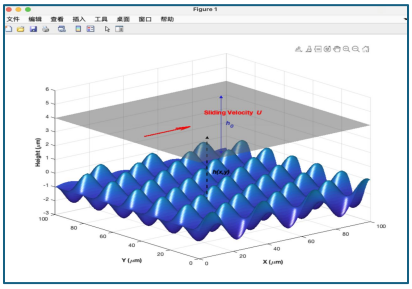

Figure 2. Micro-Contact Geometric Model of Hydrodynamic Lubrication Considering Surface Micro-Texture

To reveal the influence of surface micro-textures on lubrication performance, this paper adopts the deterministic mixed lubrication model shown in Figure 2.

2.3.1 Averaged reynolds equation

Assuming the lubricating oil is an incompressible Newtonian fluid in a steady laminar flow state, the two-dimensional Reynolds equation considering the effect of microscopic roughness is [11]:

$$\frac{\partial}{\partial x}\left(\frac{h^3}{12\eta}\frac{\partial p}{\partial x}\right) + \frac{\partial}{\partial y}\left(\frac{h^3}{12\eta}\frac{\partial p}{\partial y}\right) = \frac{U}{2}\frac{\partial h}{\partial x} \quad (7)$$

Where p is the fluid pressure, η is the dynamic viscosity, and U is the sliding velocity. The local oil film thickness equation $h(x, y)$ includes the nominal film thickness h_0 and the rough surface height $z(x, y)$:

$$h(x, y) = h_0 - z(x, y) \quad (8)$$

2.3.2 Boundary conditions and numerical methods

The equation is discretized and solved using the finite difference method on an $N_x \times N_y$ micro-grid. To handle cavitation caused by oil film rupture, the Gümbel boundary condition is applied:

$$p(x, y) = \max(p_{calculated}, 0) \quad (9)$$

2.3.3 Calculation of friction force and coefficient of friction

The fluid shear stress τ consists of the pressure flow term and the shear flow term in table 1:

$$\tau(x, y) = \frac{h}{2}\frac{\partial p}{\partial x} + \frac{\eta U}{h} \quad (10)$$

The total friction force F_f and load capacity W are obtained by integrating over the entire field, and then the friction coefficient μ is calculated:

$$F_f = \iint_A |\tau|\, dxdy, \quad \mu = \frac{F_f}{W} \quad (11)$$

Table 1. Basic Geometric and Operating Parameters for Numerical Simulation

Parameter Name	Symbol	Value and Unit
Computational Domain Size	$L_x \times L_y$	100×100μm
Grid Density	$N_x \times N_y$	256×256
Sliding Velocity	U	10m/s
Dynamic Viscosity of Lubricating Oil	η	0.05Pa s
Nominal Oil Film Thickness	h_0	1.5μm

3. Results and Discussion

3.1 Topographical Features and Functional Parameters of the Optimized Surface

Figure 3 shows the generated optimized surface (S_{sk}=-1, $S_{ku} = 4$) and its overall performance. As can be seen from the Abbott-Firestone curve in Figure 3(b), this surface exhibits a significant "tailing" feature, and the R_{vk} red-marked region indicates the presence of numerous deep valleys on the surface. These deep valleys act as "secondary lubrication sources" in micro-hydrodynamics. To further evaluate its comprehensive performance, this surface was imported into the lubrication model for solving, and the resulting micro-hydrodynamic pressure field distribution is shown in Figure 4. The pressure field distribution in Figure 4 indicates that the hydrodynamic pressure is mainly established on the intersecting ridges of the texture. Meanwhile, combined with the comprehensive simulation data in Table 2, the maximum peak pressure (P_{max}) of this surface reaches 824.2 MPa, proving that the surface has the ability to bear high contact stress.

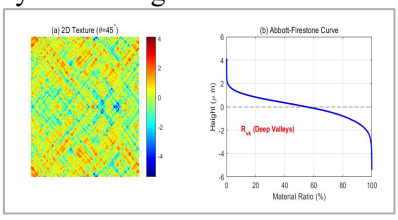

Figure 3. Micro-Topography and Bearing Area Curve of the Optimally Designed Surface

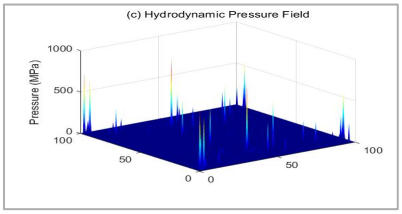

Figure 4. Micro-Hydrodynamic Pressure Field Distribution of the Optimized Surface

Table 2. Core Statistical Parameters and Lubrication Performance Indicators of the Optimized Surface

Performance and Statistical Indicators	Parameter Symbo	Value and Unit
Surface Skewness	S_{sk}	-1.0
Surface Kurtosis	S_{ku}	4.0
Friction Coefficient	μ	2.6901
Peak Pressure	P_{max}	824.2 MPa
Hydrodynamic Load Capacity	W	0.0111 N

3.2 Statistical Analysis of the Sensitivity of Load Capacity to Texture Angle

Considering the randomness of rough surface generation, a single numerical experiment may introduce accidental errors. To obtain statistically significant laws, this study used the Monte Carlo method to perform 100 independent repeated simulations for each texture angle from 30° to 70° (a total of 600 calculations). Figure 5 shows the box plot of the load capacity distribution under different texture angles.

The statistical results reveal a clear trend: within the test interval, the average hydrodynamic load-carrying capacity increases monotonically as the texture angle θ increases. It is worth noting that the average load capacity at 70° is increased by about 41% compared to the traditional 45° design. As the texture angle approaches the transverse direction (90°), the cross-hatched texture imposes a stronger flow-restriction effect, thereby increasing the hydrodynamic pressure in the contact area. Although the theoretical load capacity at 70° is the highest, comprehensively considering frictional resistance and processing feasibility, this study recommends 60° as the optimal design angle, which maintains a relatively stable performance distribution while ensuring efficient load carrying.

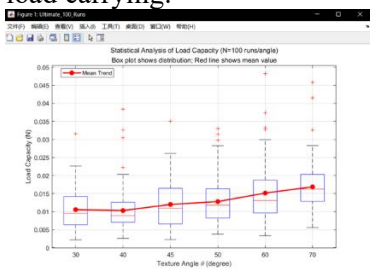

Figure 5. Statistical Analysis of Load Capacity with Texture Angles based on 100 Monte Carlo Simulations

3.3 Comparison of Stribeck Performance for Different Surface Topographies

Figure 6 compares the load-carrying performance of the optimized surface (red line) and the conventional Gaussian surface (black line) under different film thicknesses. An interesting physical phenomenon can be observed: under full-film lubrication conditions, the hydrodynamic load capacity of the ordinary Gaussian surface is slightly higher than that of the optimized surface. This is because the negative skewness deep valleys present on the optimized surface act as "pressure release channels" to a certain extent, leading to a slight decrease in the average fluid pressure. However, this sacrifice is worthwhile. Combined with the Abbott curve in Figure 3(b), the optimized surface is shown to have a large oil-storage volume (R_{vk}). When the working condition enters a mixed lubrication or starved lubrication state, the ordinary Gaussian surface will directly fail due to oil film rupture, while the optimized surface proposed in this study can rely on the stored oil in the deep valleys to maintain lubrication. This characteristic is of great significance in engineering practice, especially for heavy-duty diesel engine cylinder liners. When the piston moves to the top dead center, the sliding velocity approaches zero and the burst pressure is extremely high, making oil film rupture highly probable. The optimized deep valley feature ($S_{sk} = -1$) in this paper acts as a "micro oil reservoir" at this moment, releasing lubricating oil to the contact area through the squeeze effect, thereby effectively avoiding the "cylinder scoring" fault caused by direct metal contact. Therefore, this design scheme significantly improves the anti-interference robustness and service life of the friction pair on the premise of ensuring basic load capacity. The detailed performance comparison parameters of the two surfaces are shown in Table 3.

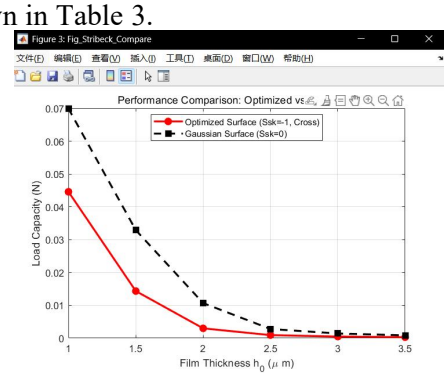

Figure 6. Comparison of Load-Carrying Performance between the Optimized Surface and the Ordinary Gaussian Surface under Different Film Thickness Conditions

Table 3. Tribological Performance Comparison between Ordinary Gaussian Surface and Non-Gaussian Cross-Hatched Surface

Performance Indicator	Ordinary Gaussian Surface	Optimally Designed Surface	Performance Improvement / Remarks
Surface Statistical Features	$S_{sk} = 0, S_{ku} = 3$	$S_{sk} = -1, S_{ku} = 4$	Introduction of deep valley oil storage features
Texture Angle	None (Isotropic)	60° (Cross-hatched)	Enhanced hydrodynamic effect
Oil Retention Capacity (R_{vk})	Low	Extremely High	Prevention of starved dry friction
Load Capacity Performance	Depends solely on film thickness	Dual mechanism of hydrodynamic pressure + oil storage	Stronger robustness

4. Conclusions

This study established a numerical-simulation-based framework for the surface topography optimization of key friction pairs such as internal combustion engine cylinder liners. By integrating a non-Gaussian random-field generation algorithm with a deterministic hydrodynamic lubrication model, the effects of surface statistical features on hydrodynamic lubrication performance were systematically investigated. The main conclusions are as follows:

(1) A hybrid surface-generation method based on the Johnson transformation system and FFT filtering was validated for engineering surface reconstruction. The method successfully reproduced the typical plateau–deep-valley topography of plateau-honed surfaces and accurately matched the target non-Gaussian distribution, providing a reliable geometric basis for tribological performance prediction.

(2) Surface skewness was identified as the dominant parameter governing load-carrying performance, with an optimal value of $S_{sk} \approx -1.0$. At this condition, the surface achieved a favorable balance between hydrodynamic action and oil-retention capacity. A moderate

kurtosis ($S_{ku} \approx 4.0$) urther enhanced the micro-hydrodynamic effect, whereas excessively high kurtosis increased local contact pressure and the risk of surface fatigue.

(3) Texture orientation had a significant influence on lubrication performance. At a sliding speed of 10 m/s, the 60°cross-hatched texture exhibited higher load-carrying capacity than the conventional 45°design. Although the optimized non-Gaussian surface showed slightly lower steady-state load capacity than a Gaussian surface under full-film lubrication, its larger reduced valley depth (R_{vk}) produced a pronounced micro-oil-reservoir effect, resulting in better anti-scuffing robustness under mixed and starved lubrication conditions.

Overall, the proposed framework enables decoupled and precise evaluation of individual statistical parameters without relying on physical prototypes, and provides useful guidance for the surface-texture design of high-performance engine friction pairs.

References

[1] Lyu Y J, Luo H B, Zhang Y F, Kang J X, Li P Z. Research progress of surface technology in piston assembly-cylinder liner system of internal combustion engines. Journal of Traffic and Transportation Engineering, 2022, 22(1):24-41.

[2] Yuan P Q, Fang J T, Wang L Q, Liang H, Fu X L. Research on tribological properties of metal components. Manufacturing Technology & Machine Tool, 2024, (5):114-121.

[3] Ma S, Liu Y, Wang Z, Wang Z, Huang R, Xu J. The Effect of Honing Angle and Roughness Height on the Tribological Performance of CuNiCr Iron Liner. Metals, 2019, 9(5):487.

[4] Zhu S, Zhang X, Sun J, Wang D. Average Flow Model for Micropolar Fluid Lubrication of Rough Surface Bearings. Journal of Mechanical Engineering, 2024, 60(7):203-211.

[5] Grabon W, Pawlus P, Sep J. Tribological characteristics of one-process and two-process cylinder liner honed surfaces under reciprocating sliding conditions. Tribology International, 2010, 43(10):1882-1892.

[6] Sedlaček M, Podgornik B, Vižintin J. Influence of surface preparation on roughness parameters, friction and wear. Wear, 2009, 266(3):482-487.

[7] Tong D H, Yin B F, Xu B, Fu Y H, Hua X J, Huang G L. Research on tribological performance of the partition discriminating textured cylinder liner. Transactions of CSICE, 2021, 39(5):451-458.

[8] Liu L, Zhang X, Wan X, Zhou S, Gao Z. Digital twin-driven surface roughness prediction and process parameter adaptive optimization. Advanced Engineering Informatics, 2022, 51:101470.

[9] Ma J, Fu C, Zhang H, Chu F, Shi Z, Gu F, Ball A D. Modelling non-Gaussian surfaces and misalignment for condition monitoring of journal bearings. Measurement, 2021, 174:108983.

[10] Chen J, Tang J, Shao W, Li X, Yang D, Zhao B, Dong H. A new numerical simulation method of 3D rough surface topography with coupling 3D roughness parameters Sdr, Sdq, Spd, Spc, and characteristic functions. Tribology International, 2024, 200:110117.

[11] Pere B, Lénárt M. Advancing Lubrication Modeling: A Preliminary Study of Finite Element Solutions for Cavitation-Aware Reynolds Equation. Engineering Proceedings, 2025, 113(1):2.

